

Enhanced detection of acousto-photonic scattering using a photorefractive crystal

Lei Sui^a, Todd Murray^{*a}, Gopi Maguluri^a, Alex Nieva^b, Florian Blonigen^b, Charles DiMarzio^{†b} and Ronald A. Roy^{‡a}

Center for Subsurface Sensing and Imaging Systems

^aDepartment of Aerospace and Mechanical Engineering, Boston University,
110 Cummington Street, Boston, MA, 02215, USA

^bDepartment of Electrical and Computer Engineering, Northeastern University,
360 Huntington Avenue, Boston, MA, 02115, USA

ABSTRACT

Acousto-photonic imaging (API) is a dual-wave sensing technique in which a diffusive photon wave in a turbid medium interacts with an imposed acoustic field that drives scatterers to coherent periodic motion. A phase-modulated photon field emanates from the interaction region and carries with it information about the local opto-mechanical properties of the insonated media. A technological barrier to API has been sensitivity – the flux of phase-modulated photons is very small and the incoherence of the resulting speckle pattern reduces the modulation of the scattered light leading to low sensitivity. We report preliminary results from a new detection scheme in which a photorefractive crystal is used to mix the diffusively scattered laser light with a reference beam. The crystal serves as a dynamic holographic medium where the signal beam interferes with the reference beam, creating a photorefractive grating from which beams diffract. In addition, the phase modulation is converted to an amplitude modulation so that the API signal can be detected. Measurements of the API signal are presented for gel phantoms with polystyrene beads used as scatterers, showing a qualitative agreement with a simple theoretical model developed.

Keywords: Acousto-photonic imaging, photorefractive crystal, sensitivity, turbid medium

1. INTRODUCTION

A number of optical imaging techniques¹ have been investigated for biomedical imaging based on differences in the optical properties of different tissue types. The main difficulty in implementing such optical methods is that light is highly scattered in biological tissue. This prevents the scattered light from yielding good spatial resolution. In an attempt to address this limitation, ultrasonic techniques are “combined” with purely optical techniques², as ultrasonic waves scatter much less readily in biological tissue and offer sub-millimeter resolution even at depth. Among these hybrid methods is a technique we refer to as “acousto-photonic imaging” (API)³. This technique falls under a number of different names depending on the background and perspective of the investigator: “ultrasound tagging of light” (UTL; Marks *et al.*⁴, Mahan *et al.*⁵), “acousto-optic tomography” (AOT; Kempe *et al.*⁶), “acousto-optic imaging” (AOI; Leveque *et al.*⁷), and “ultrasound-modulated optical tomography” (UMOT; Wang and Zhao⁸). Regardless of the differences of these terms, the physical concept behind them is the same: ultrasound beams are used to modulate diffuse light, yielding spatially resolved opto-mechanical information. This combined technique retains the benefits of both the optical and ultrasonic techniques, i.e., it can reveal the physiological information about biological tissue while maintaining ultrasonic resolution, for the API interaction region is defined by the dimensions of the ultrasonic beam and/or the focal spot size.

Further author information:

* Prof. Todd Murray, Email: twmurray@bu.edu; Phone: 617-353-3951;

† Prof. Charles A. DiMarzio, Email: dimarzio@ece.neu.edu; Phone: 617-373-2034;

‡ Prof. Ronald A. Roy, Email: ronroy@bu.edu; Phone: 617-353-4846.

Marks *et al.*⁴ first reported the modulation of light with focused, pulsed ultrasound in a homogeneous, scattering media in 1993. This was closely followed by the work of Wang *et al.*⁹ and Kempe *et al.*⁶ who demonstrated the utility of using the tagging of diffuse photons for imaging purposes. The former group developed ultrasonic modulated optical tomography using a CW ultrasound transducer and a CW laser source. The signals were detected using a single PMT detector. Wang and Ku¹⁰ later introduced a technique in which the ultrasonic source is chirped, thereby encoding spatial information on the transmitted laser light and allowing for 1-D scans along the ultrasonic axis to be produced from a single time domain waveform. Conventional single detector techniques that have been used result in extremely low light levels when the detection aperture is limited to single speckle detection and reduced modulation depth when the detection aperture is increased to receive multiple speckles. In 1999, Leveque *et al.*¹¹ presented a new approach to detect the modulated signals using a 256x256 element CCD array. In their technique, the speckle size is adjusted to approximately match the size of a single element of the CCD array and the modulation amplitude at each pixel is measured using a lock-in detection scheme. The amplitudes measured at each pixel element are subsequently summed leading to a substantial signal-to-noise ratio increase over single element detection, and the authors demonstrated the detection of absorbing objects buried in biological tissue (turkey breast). Yao *et al.*¹² combined the multiple speckle detection technique with their frequency swept technique and obtained 2D images of multiple objects buried in biological tissue. Selb *et al.*¹³ have measured the signals produced at the second harmonic of the acoustic source leading to improved spatial resolution.

In this work we present a new approach for the detection of modulated light in acousto-photonics imaging using a photorefractive crystal (PRC) based system. PRC-based interferometers have seen relatively widespread use in the optical detection of ultrasound in nondestructive evaluation and materials characterization applications¹⁴⁻¹⁷. These systems are ideally suited for ultrasound detection off of optically rough surfaces. In such a system, the signal beam passes through or is reflected off of the target material acquiring a phase modulation in the presence of ultrasound. The signal beam is then sent to the PRC where it is mixed with a reference beam (or pump beam), directly derived from the laser source. An interference pattern is formed in the crystal exciting free carriers in the bright regions which drift or diffuse to the dark regions leading to a space charge field formation. The index of refraction is modulated through the electro-optic effect, and the reference beam is diffracted off of this grating into the signal beam direction in the two-wave mixing process. The diffracted reference beam phase front replicates that of the signal beam providing a local oscillator (LO) for interferometric detection. The diffracted reference beam and transmitted signal beam interfere at the photodetector where any phase modulation encoded on the signal beam is converted to an intensity modulation which is observed at the photodetector. Note that the PRC is adaptive in that the index grating is continually “rewritten” on the time scale of the PRC response time, while high frequency modulation produced by the ultrasonic source is not compensated for, producing a relative phase shift between the signal and reference beams (and intensity change at the detector). An external field can be applied to enhance the TWM gain and then the detection sensitivity^{17,18}.

In this paper, the PRC-based system is applied to the detection of acoustically modulated, diffuse scattered light for the first time. A simple mathematical model is developed to explain the nature of the detected optical signal. The experimental setup is described in detail, including a description of the focused ultrasound beam and the fabrication of our API tissue-mimicking phantom. Preliminary experimental results are presented and qualitatively compared with the model predictions.

2. PRC-BASED DETECTION OF API SIGNALS

Consider the case of two plane waves interfering within a photorefractive crystal as illustrated in Figure 1. The signal beam amplitude is represented by $E_s(x=0,t)$ at the entrance to the PRC and $E_s(x=D,t)$ at the exit of the PRC, where D is the thickness of the crystal. We assume that the signal beam is phase modulated at a frequency sufficiently high that the PRC response time is large with respect to the oscillation period. The signal beam is amplified as it propagates through the crystal with a two wave mixing gain of γ as the reference beam is diffracted into the signal beam direction. The diffracted reference beam has the same phase front as the transmitted signal beam, but does not acquire the high frequency phase modulation. Note that the gain coefficient is complex and the diffracted reference beam may be uniformly shifted in phase with respect to the signal beam. The gain coefficient is given by $\gamma = \gamma' + i\gamma''$, where γ' is the real part of the gain and γ'' is the imaginary part. The optical absorption coefficient in the crystal is given by α . In the

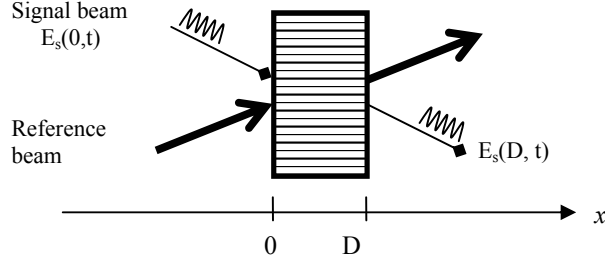


Fig. 1. The TWM configuration of a PRC with length D : a signal beam $E_s(0,t)$ becomes $E_s(D,t)$ after passing through the index of refraction grating formed by the interference of the signal beam and the reference beam.

case where the reference beam intensity is large compared to the signal beam (i.e., undepleted pump approximation), the amplitude of the transmitted signal beam may be written as¹⁹:

$$E_s(D,t) = \exp(-\alpha D / 2) E_s(0,0) \{ [\exp(\gamma D) - 1] + \exp(i\phi_a \sin \omega_a t) \} \quad (1)$$

The first term in the bracket represents the diffracted reference beam while the second term corresponds to the transmitted signal beam, where ϕ_a and ω_a are the amplitude and the angular frequency of the phase modulation, respectively. The intensity follows from Eq. (1):

$$I_s(D,t) = \exp(-\alpha D) I_s(0,0) \{ |e^{\gamma D} - 1|^2 + 1 + 2 \operatorname{Re}[(e^{\gamma D} - 1) * \exp(i\phi_a \sin \omega_a t)] \}, \quad (2)$$

where $I_s(0,0) = |E_s(0,0)|^2$ and “*” denotes the complex conjugate.

We can expand Eq. (2) in terms of its DC and AC components, using Bessel functions and retaining the lowest-order terms²⁰:

$$I_{DC}(D,t) = \exp(-\alpha D) I_s(0,0) \{ |e^{\gamma D} - 1|^2 + 1 + 2[e^{\gamma D} \cos(\gamma D) - 1] J_0(\phi_a) \}; \quad (3)$$

$$I_{AC}(D,t) = 4 \exp(-\alpha D) I_s(0,0) e^{\gamma D} \sin(\gamma D) J_1(\phi_a) \sin(\omega_a t). \quad (4)$$

Eq. (3) tells us that, in addition to the AC modulation given by Eq. (4), the intensity of the signal beam after passing through the PRC has an additional time-independent (i.e. DC) offset which is proportional to the amplitude of the optical phase modulation induced by the ultrasound. It is noted that the above expressions correspond to a signal beam incident on the PRC with a fixed, time dependent phase modulation corresponding to a single optical path. In the case of API signal detection in highly scattering media, light travels over multiple paths and the AC component of the signal observed at a single detector is the summation of the signals from each of the paths. As the modulation induced by the ultrasound is not uniform spatially, it is not expected that the AC components of the signals will add coherently at the detector. The DC component, subsequently referred to as the “DC offset”, depends only on the amplitude of the phase modulation and thus allows for the measurement of the magnitude of the mean phase shift induced by the ultrasound on the multiply scattered optical field. Experimentally, it is observed that the DC offset signal is substantially larger than the AC component in diffuse media. In order to maximize the DC offset signal, a PRC detection configuration is chosen in which the diffracted reference beam is in phase with the transmitted signal beam giving pure (real) photorefractive gain. It should be mentioned that ϕ_a is related to the acoustic driving pressure. However, the precise nature of this relationship is not known at this time.

3. EXPERIMENTAL SETUP

The experimental setup based on the PRC-detector is shown in Fig. 2 above. The system has four main components: the acoustic source, the optical source, PRC-detector, and the signal sensing/processing/recording instrumentation.

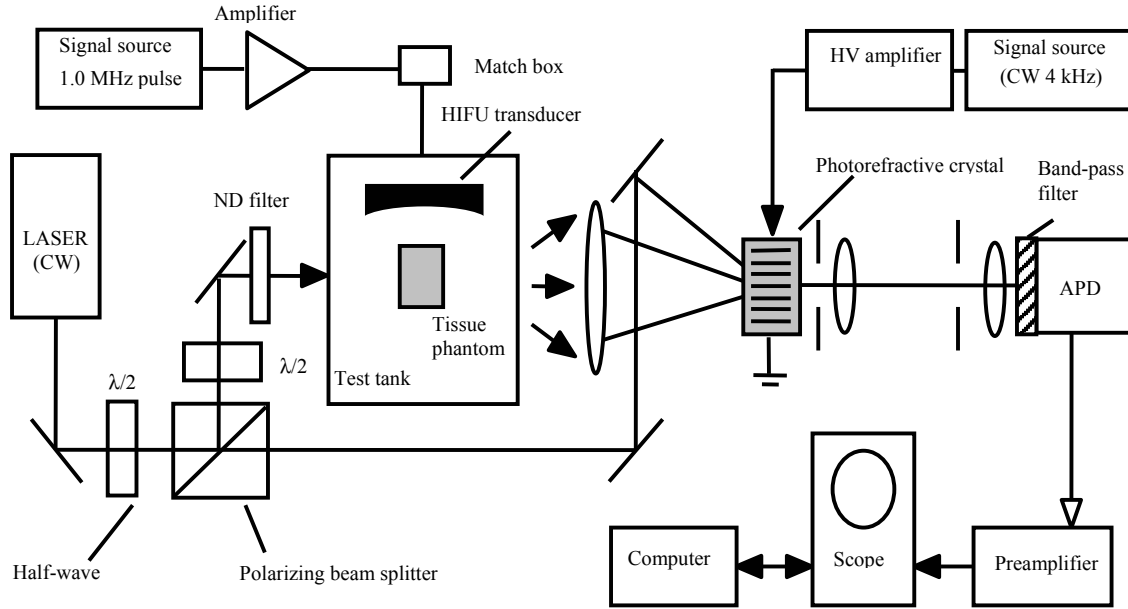


Fig. 2. The experimental setup for PRC-based acousto-photonic imaging

The sound source is an unbacked, single-element, spherically focused, piezoelectric transducer (Sonic Concepts, H101, Woodinville, WA). This transducer has a 6.32-cm focal distance (measured in degassed water at 28°C) and a 7.0-cm aperture. The center frequency of the transducer is 1.1 MHz and the bandwidth is 0.85-1.35 MHz. We calibrated the source at 1 MHz in degassed water using a PVDF needle hydrophone (Precision Acoustics Ltd, SN693, Dorchester, UK). The focal region, defined by the full width of half maximum intensity (FWHM), is a cigar-shaped ellipsoid with a long axis of about 9 mm and a short axis of about 1.5 mm. In our experiments we typically employ 20-cycle pulses with a pulse repetition frequency (PRF) of 100 Hz. This pulse train is produced by a standard function generator whose sync output is used to externally trigger the digital oscilloscope. The resulting acoustic drive signal is amplified by a fixed-gain power amplifier (ENI, A150, Rochester, NY), and is then sent to the impedance matching box before driving the transducer. The source is used to insonify a tissue-mimicking gel phantom that is submerged in a small tank of degassed, filtered, and deionized water. The tank dimensions are 30cm×30cm×20cm (L×W×H) and glass walls are employed for optical access. Acoustical access is achieved via the free water surface, with the beam projected vertically downward.

We employ a diode-pumped, 532-nm wavelength Nd:YAG laser with 80-mW (CW) output power and a 0.32-mm diameter beam. The unit delivers a linearly polarized Gaussian beam, which is sent to a variable beamsplitter (half waveplate/ polarizing beamsplitter) and split into a signal beam and reference beam. The reference beam is directed around the test tank and sent directly to the PRC. The signal beam is sent through a half waveplate and is delivered to the submerged tissue-mimicking phantom via the flat glass walls of the tank. A neutral density (ND) wheel is employed so that an adjustable signal beam power is achieved in the experiment and to avoid saturating the APD when tissue phantoms with low scattering are used. The scattered and ultrasonically modulated light is collected by a lens after the tank and is directed into the PRC where it interferes with the reference beam. Our PRC-detector employs a BSO crystal (MolTech GmbH, Berlin, Germany) with dimensions of 5mm×5mm×7mm, and a holographic cut along the [001], [110] and $[1\bar{1}0]$ directions. A 4 kHz AC field of 10-kV/cm peak-to-peak high voltage is applied to the crystal using a high voltage amplifier in order to enhance the two-wave mixing gain. After the signal beam passes through the PRC, a pair of apertures is used to prevent any reference beam light scattered by the edges of the PRC from reaching the

detector. Two lenses serve to collect the signal beam light after passing through the PRC and focus it onto an avalanche photodiode (APD) (Advanced Photonix, 394-70-74-661, Camarillo, CA). A laser line bandpass filter (Newport, 10LF10-532, Irvine, CA) eliminates all ambient light.

4. FABRICATION OF THE API PHANTOM

API is a hybrid process that involves both light and sound propagation. Thus we seek a test media that mimics both the acoustical and optical properties of human tissue. The relevant acoustical properties of human tissue include density, speed of sound and the attenuation coefficient. The important optical properties include the scattering coefficient and absorption coefficient. As one of the ultimate applications of API imaging is for the detection of breast cancer and since breast tissue has an optical absorption coefficient that is small compared to the scattering coefficient²¹, we set out to develop phantoms that replicate the reduced scattering coefficient (optical descriptor), and the density and speed of sound (acoustical descriptors) of living tissue. We make no attempt to recreate the micro-architecture or vasculature of real tissue at this point in time.

Our API phantom is a modification of the transparent acrylamide gel phantom described in references 22 and 23 with the addition of $0.4\ \mu\text{m}$ -diameter polystyrene microspheres for optical diffusivity. The concentration of particles required to generate a desired optical diffusivity is determined using a standard from a Mie scattering formulation²⁴. The fabrication procedure is as follows:

- (1) 9.375 g of acrylamide and 0.265 g of bis-acrylamide are dissolved in 50 ml of deionized water.
- (2) The mixture is stirred and degassed for approximately 10 minutes.
- (3) The desired amount of microspheres are added to the mixture and the mixture is slowly stirred to avoid entraining bubbles.
- (4) 0.02g of ammonium persulfate (a polymerizing initiator) and 0.2 ml of TEMED (Sigma Chemical) are added to the mixture and the fluid-like mixture is quickly poured into a mold.
- (5) The mold is covered and the mixture is allowed to cure for approximately 10 hours at room temperature until it is completely solidified.
- (6) The phantom is thoroughly rinsed with water and subsequently stored submerged in water. (It is noted that unpolymerized acrylimide is highly toxic and proper precautions must be taken during phantom preparation.)

The dimensions of the phantoms used in this work are about $4.3\text{cm} \times 4.3\text{cm} \times 2.9\text{cm}$ and they are oriented such that the laser passes through the 2.9-cm dimension. The measured acoustic properties of the phantom material are listed in Table 1 in comparison with literature values for human breast tissue. The obvious mismatch in acoustic attenuation is not deemed significant to the work reported herein.

Acoustic Properties	Gel Phantom	Human Breast
Mass Density (Kg/m^3)	1045	990-1060 ²¹
Speed of Sound (m/s)	1515	1450-1570 ²⁵
Attenuation ($\text{Np}/\text{m}/\text{MHz}$)	0.2	3.4-7.4 ²¹

Table 1: Measured and literature values for the acoustic properties of human breast tissue

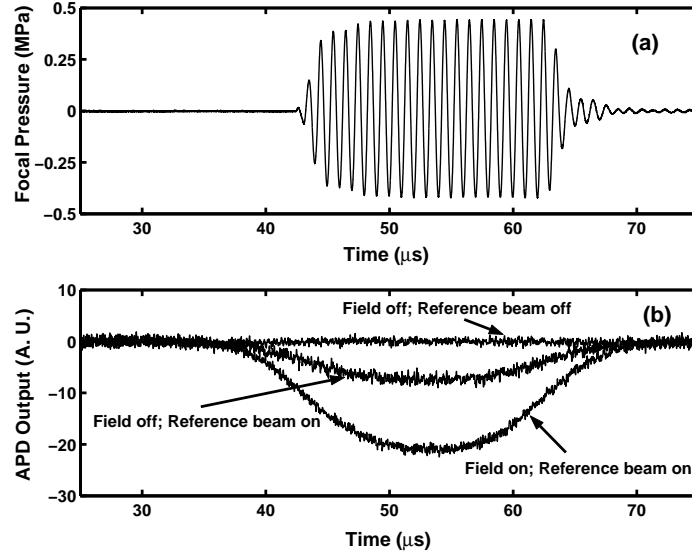


Fig. 3. A typical offset signal (b) enhanced by both the high-voltage field and the reference beam under the corresponding focal pressure (a) for the phantom with a reduced scattering coefficient of 3 cm^{-1} .

5. EXPERIMENTAL RESULTS AND DISCUSSION

Figure 3(a) shows the measured focal pressure generated by the sound source driven by a 20-cycle pulse at 1 MHz center frequency. The peak pressure in this plot is approximately 0.4 MPa. The corresponding API signals generated in a phantom with a reduced scattering coefficient of $\mu_s' = 3 \text{ cm}^{-1}$ and detected with the PRC-based scheme are illustrated in Fig. 3(b). There are a few important points to note regarding these waveforms. The top trace in Fig. 3(b) shows the signal detected in the absence of a reference beam to the PRC. In this case, the PRC has no effect (except for absorbing a small amount of the signal beam) and the light collected from the phantom is sent directly to the APD. We do not observe any signal in this case. In the other traces in the figure, the reference beam is present. In the lower trace, with highest signal amplitude, the AC field is also applied to the crystal and serves to increase the two wave mixing gain. In both of the cases with a reference beam present there is no signal detected at the 1 MHz ultrasonic frequency, but rather a signal that follows the envelope of the pulse train. This is the “DC offset” signal that is described by Eq. 4. One can readily see that the PRC-induced mixing of the signal beam and the reference beam, facilitated by the addition of a high voltage AC bias field, dramatically enhances the offset signal, which in turn tracks the envelope of the acoustic pulse in the time domain. Note that in the current configuration, the diffracted reference beam is in phase with the transmitted signal beam such that the gain is purely real and thus we do not expect to see the 1 MHz modulation (see Eq. 3). However, using polarization optics we also put the diffracted reference beam in quadrature with the transmitted signal beam and still observed a 1 MHz signal that was negligible with respect to the DC offset signal presented above. The data shown in Fig. 3(b) corresponds to a simple coherent average of 1000 individual waveforms. It is not necessary to employ lock-in detectors or complicated demodulation schemes. Moreover, the use of coherent averaging in the time domain admits the use of acoustic pulses rather than CW ultrasound – a significant advantage for it allows for spatial resolution along the axis of the sound source and it minimizes deleterious thermal bioeffects that can result from high-intensity ultrasound exposure.

Fig. 4 shows the detected API signal for the same driving pressure as shown in Fig. 3(a) but generated in a transparent phantom. It is evident that this signal is the linear sum of two components: an AC component at the ultrasound frequency and a DC component that tracks the envelope of the acoustic pulse. This is in a qualitative agreement with what our model prediction; see Eqs. 3 and 4. In this case, the presence of a small AC component indicates that the gain is not purely real but rather has a small imaginary component such that Eq. 4 does not go to zero. The absence of the AC component in Fig. 3(b) is due to the enhanced diffusivity of that particular phantom. The AC modulated signal is

not coherent spatially over the wavefront and when the scattered light is collected to a single detector the signal modulation is greatly reduced. However, the DC signal survives and, according to Eq. 3, this “DC offset” component is *directly related to the ultrasonically induced phase shift*. It is a direct measure of the level of acousto-photonic interaction in the acoustic focal region. This is the very quantity we endeavor to image.

It is important to stress that we found it exceedingly difficult to detect the AC modulation signal in highly diffusive phantoms, particularly when using pulsed ultrasound insonation. The current state of the art in API sensing and imaging is to use this weak modulation signal as the very definition of image contrast. CW insonation and complex demodulation schemes are normally required. We believe that using a PRC-based detector to access the DC offset signal is both a more economical and more sensitive approach, particularly when applied to imaging scenarios employing long propagation paths such as deep seated tumors. The offset signal is sensitive to the total phase shift induced by ultrasound and is unaffected by spatial incoherence created by media diffusivity. One can sense signals integrated over large area detectors and thus significantly enhance sensitivity by over other single detector schemes.

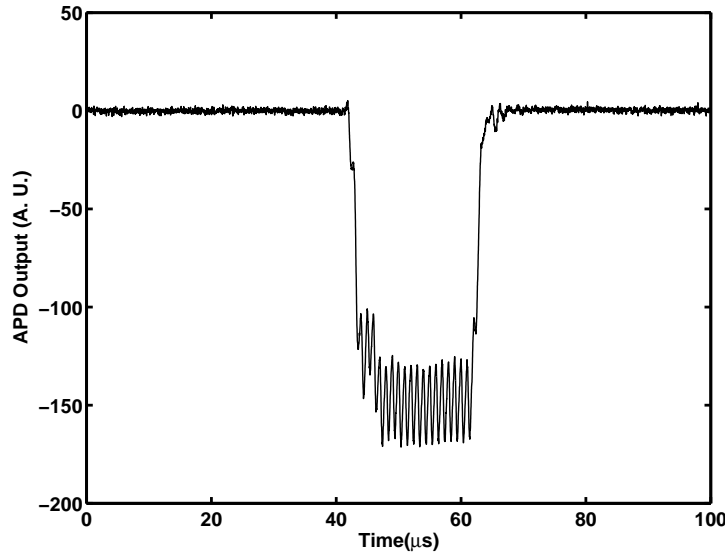


Fig. 4. The APD output for the clear phantom under the same driving pressure as shown in (a) of Fig. 3.

6. CONCLUSION

A gel-based API phantom that matches certain relevant acoustical and optical properties of tissue has been fabricated. An optical detector employing a photorefractive-crystal-based interferometer has been applied to detect the API signal induced in the phantom by the interaction of focused ultrasound and diffuse laser light. Two distinct signals were detected: a weak AC component corresponding to an intensity modulation at the ultrasound frequency riding on top of a DC offset signal that tracks the envelope of the acoustic pulse. The former is severely compromised by media diffusivity whereas the latter survives the multiple scattering process and was shown to be directly related to the total phase shift induced by the acoustic beam. A simple theoretical model was presented that exhibits qualitative agreement with the experimental results.

The “DC offset signal” is a direct measure of the strength of acousto-photonic interaction. It emanates from a volume of tissue delineated by the acoustic focal volume, thus, API imaging resolution is essentially the same as that of conventional ultrasound and significantly better than other optical techniques such as DOT. The detection of the offset signals yields improved sensitivity, making it possible to work in the time domain using pulsed ultrasound. The net gain is spatial resolution along the transducer axis and a reduced potential for thermal bio-effects.

ACKNOWLEDGEMENT

This work was supported by CenSSIS, the Center for Subsurface Sensing and Imaging Systems, under the Engineering Research Centers Program of the National Science Foundation (award number EEC-9986821).

REFERENCES

1. V. V. Tuchin, ed., *Handbook of Optical Biomedical Diagnostics*, SPIE, Washington, 2002.
2. A. A. Oraevsky, ed., *Proceedings of SPIE 4960 Biomedical Optoacoustics IV*, SPIE, Washington, 2003.
3. C. A. DiMarzio, R. J. Gaudette and T. J. Gaudette, "A New Imaging Technique Combining Diffusive Photon Density Waves and Focussed Ultrasound", *Proc. SPIE* **3597**, 376-384, 2000.
4. F. A. Marks, H. W. Tomlinson and G. W. Brooksby, "A comprehensive approach to breast cancer detection using light: photon localization by ultrasound modulation and tissue characterization by spectral discrimination", *Proc. SPIE* **1888**, 500-510, 1993.
5. G. D. Mahan, W. E. Engler, J. J. Tiemann and E. Uzgiris, "Ultrasonic tagging of light: Theory", *Proc. Natl. Acad. Sci. USA* **95**, 14015-14019, 1998.
6. M. Kempe, M. Larionov, D. Zaslavsky and A. Z. Genack, "Acousto-optic tomography with multiply scattered light", *J. Opt. Soc. Am. A* **14**, 1151-1158, 1997.
7. S. Leveque, J. Selb, L. Pottier and A. C. Boccara, "In situ local tissue characterization and imaging by backscattering acousto-optic imaging", *Opt. Comm.* **196**, 127-131, 2001.
8. L. Wang and X. Zhao, "Ultrasound-modulated optical tomography of absorbing objects buried in dense tissue-simulating turbid media", *Appl. Opt.* **36**, 7277-7282, 1997.
9. L. Wang, S. L. Jacques and X. Zhao, "Continuous-wave ultrasonic modulation of scattered laser light to image objects in turbid media", *Opt. Lett.* **20**, 629-631, 1995.
10. L. Wang and G. Ku, "Frequency-swept ultrasound-modulated optical tomography of scattering media", *Opt. Lett.* **23**, 975-977, 1998.
11. S. Leveque, A. C. Boccara, M. Lebec and H. Saint-Jalmes, "Ultrasonic tagging of photon paths in scattering media: parallel speckle modulation processing", *Opt. Lett.* **24**, 181-183, 1999.
12. G. Yao, S. Jiao and L. Wang, "Frequency-swept ultrasound-modulated optical tomography in biological tissue by use of parallel detection", *Opt. Lett.* **25**, 734-736, 2000.
13. J. Selb, L. Pottier, A. C. Boccara, "Nonlinear effects in acousto-optic imaging", *Opt. Lett.* **27**, 918-920, 2002.
14. R. K. Ing and J. P. Monchalin, "Broadband optical detection of ultrasound by two-wave mixing in a photorefractive crystal", *Appl. Phys. Lett.* **59**, 3233-3235, 1991.
15. A. Blouin and J. P. Monchalin, "Detection of Ultrasonic Motion of a Scattered Surface by Two-Wave Mixing in a Photorefractive GaAs Crystal", *Appl. Phys. Lett.* **65**, 932-934, 1994.
16. P. Delaye, A. Blouin, L. Montmorillon, I. Biaggio, D. Drolet and J. Monchalin and G. Roosen, "Detection of ultrasonic vibrations on rough surfaces through the photorefractive effect", *Proc. SPIE* **2782**, 464-485, 1996.
17. T. W. Murray, H. Tuovinen and S. Krishnaswamy, "Adaptive optical array receivers for detection of surface acoustic waves", *Appl. Opt.* **39**, 3276-3284, 2000.
18. P. Delaye, A. Blouin, D. Drolet, L. Montmorillon, G. Roosen and J. Monchalin, "Detection of ultrasonic motion of a scattering surface by photorefractive InP: Fe under an applied dc field", *J. Opt. Soc. Am. B* **14**, 1723-1734, 1997.
19. P. Delaye, L. A. Montmorillon and G. Roosen, "Transmission of time modulated optical signals through an absorbing photorefractive crystal", *Opt. Comm.* **118**, 154-164, 1995.
20. D. Shoemaker, R. Schilling, L. Schnupp, W. Winkler, K. Maischberger, and A. Rudiger, "Noise behavior of the Garching 30-meter gravitational-wave detector", *Phys. Rev. D* **38**, 423-432 1988.
21. F. A. Duck, *Physical Properties of Tissue*, Academic Press, San Diego, CA, 1990.
22. John A. Viator and Scott A. Prael, "Photoacoustic imaging of gelatin phantoms using matched field processing", *Proc. SPIE* **3601**, 276-283, 1999.
23. U. S. Sathyam and S. A. Prael, "Limitations in measurements of subsurface temperatures using pulsed photothermal radiometry", *J. Biomed. Opt.* **2**, 251-261, 1997.
24. URL: http://omlc.ogi.edu/calc/mie_calc.html.
25. G. Kossoff, E. K. Fry and J. Jellins, "Average velocity of ultrasound in the human female breast", *J. Acoust. Soc. Am.* **53**, 1730-1736, 1973.